Available online at www.sciencedirect.com
SCIENCE DIRECT®
Medical Laser Application 20 (2005) 207–216
Medical Laser Application
www.elsevier.de/mla

Femtosecond pulse-induced microprocessing of live *Drosophila* embryos

Willy Supatto[a], Delphine Débarre[b], Emmanuel Farge[a], Emmanuel Beaurepaire[b,*]

[a]*Laboratory of Physico-Chemistry of Life, Institute Curie, Centre National de la Recherche Scientifique UMR 168, F-75248 Paris, France*
[b]*Laboratory for Optics and Biosciences, Centre National de la Recherche Scientifique UMR 7645, Institut National de la Santé et la Recherche Médicale U696, Ecole Polytechnique, F-91128 Palaiseau, France*

Received 17 June 2005; accepted 5 July 2005

Abstract

We characterized the effect of femtosecond pulse trains on gastrulating *Drosophila* embryos using two-photon-excited fluorescence (2PEF) and third-harmonic generation (THG) microscopy. Femtosecond pulses can be used to perform controlled intravital microdissections that alter the embryo structural integrity but do not significantly perturb cytoskeleton dynamics in adjacent cells. Such targeted ablations can be used to remotely perturb cell movements in developing embryos. The transparent combination of femtosecond pulse-induced ablation with nonlinear microscopy can be used to analyze in vivo the effect of cell and tissue deformations.

Keywords: Femtosecond pulse-induced ablation; Two-photon-excited fluorescence microscopy; Third-harmonic generation microscopy; *Drosophila* embryo development

Introduction

Femtosecond near-infrared (NIR) lasers are progressively becoming familiar to life scientists owing to the success of multiphoton microscopy (MPM) [1], a technique now considered the best means for high-resolution fluorescence imaging in intact tissues or live animals [2]. Two-photon-excited fluorescence (2PEF) microscopy – the most common form of MPM – has found applications in in vivo studies in neuroscience [3–5], physiology [6,7] and developmental biology [8]. Besides 2PEF, other nonlinear optical processes are being explored as contrast mechanisms, such as second- [2,9] and third-harmonic generation (THG) [10], or coherent anti-Stokes Raman scattering [11,12]. In particular, THG microscopy [10,13,14] detects optical heterogeneities and has been shown to provide detailed structural images of unstained zebrafish [15] and *Drosophila* [16] embryos.

Tightly focused higher energy pulses can also be used to perform three-dimensional ablations in biological media, because the nonlinear nature of the photodestructive effects confines them to the vicinity of the focal point, where the intensity is highest. In particular, femtosecond NIR pulses are used in corneal surgery [17,18], and are finding additional applications in neurosciences [19,20], plant biology [21], and cell biology (in vitro nanodissection of isolated chromosomes [22], cell transfection [23] or intratissue/intracellular nanodissection [24–28]).

Here we describe an application of femtosecond pulse-induced ablation in developmental biology. We used ultrashort laser pulses to perform three-dimensional microdissections inside live *Drosophila* embryos in

*Corresponding author. Fax: +33 169 333 017.
E-mail addresses: willy.supatto@curie.fr (W. Supatto), emmanuel.beaurepaire@polytechnique.fr (E. Beaurepaire).

1615-1615/$ - see front matter © 2005 Elsevier GmbH. All rights reserved.
doi:10.1016/j.mla.2005.07.001

order to locally modify their structural integrity. By tracking the outcome of the microdissections by nonlinear microscopy (2PEF and THG) using the same laser source (80 MHz, 130–200 fs pulses), we have found that local ablations can be used to modulate remote morphogenetic movements. This all-optical methodology provides a novel, non-genetic approach to study embryo morphogenesis, and provides insight into the interplay between molecular signaling – including gene expression – and tissue deformations [29].

In this manuscript, we present a physical and biological characterization of the effects of femtosecond pulses on developing embryos based on 2PEF/THG microscopy data, and we show how intravital ablations can be applied to the study of morphogenetic movements.

Materials and methods

Wild-type and transgenic fly lines

Oregon-R was used as the wild-type *Drosophila melanogaster* strain. The sGMCA transgenic line [30] expressing eGFP fused with actin-binding moesin fragments exhibits fluorescence labeling of the cytoskeleton and provides a fluorescent outline of cell shape. Another transgenic line containing eGFP fused with a nuclear localization sequence (nls-GFP, Bloomington stock center) exhibits labeling of nuclei [31]. In this study, all stages of developing *Drosophila* embryo are referred to according to [32].

Embryo preparation

Embryos were collected and selected during cellularization (developmental stage 5 [32]), dechorionated, and glued to a coverslip [33]. Finally, embryos were covered and maintained in Phosphate-Buffered Saline (PBS) at room temperature ($19 \pm 1\,^{\circ}C$) during ablation and imaging. Large working distance objectives were used to prevent embryo hypoxia.

Nonlinear (2PEF and THG) microscopy

Imaging was performed on a nonlinear scanning upright microscope (Fig. 1) incorporating a femtosecond titane:sapphire (Ti:S) oscillator (Coherent), an optical parametric oscillator (OPO, APE, Germany), galvanometer mirrors (GSI Lumonics), water-immersion objectives (60×0.9NA and 20×0.95NA, Olympus), photon-counting photomultiplier modules (Electron Tubes), and lab-designed 100 MHz counting electronics. A motorized beam attenuator consisting of a half-wave plate and a Glan polarizer allowed injecting up to 90% of the Ti:S beam either into the OPO for THG imaging, or directly into the microscope for

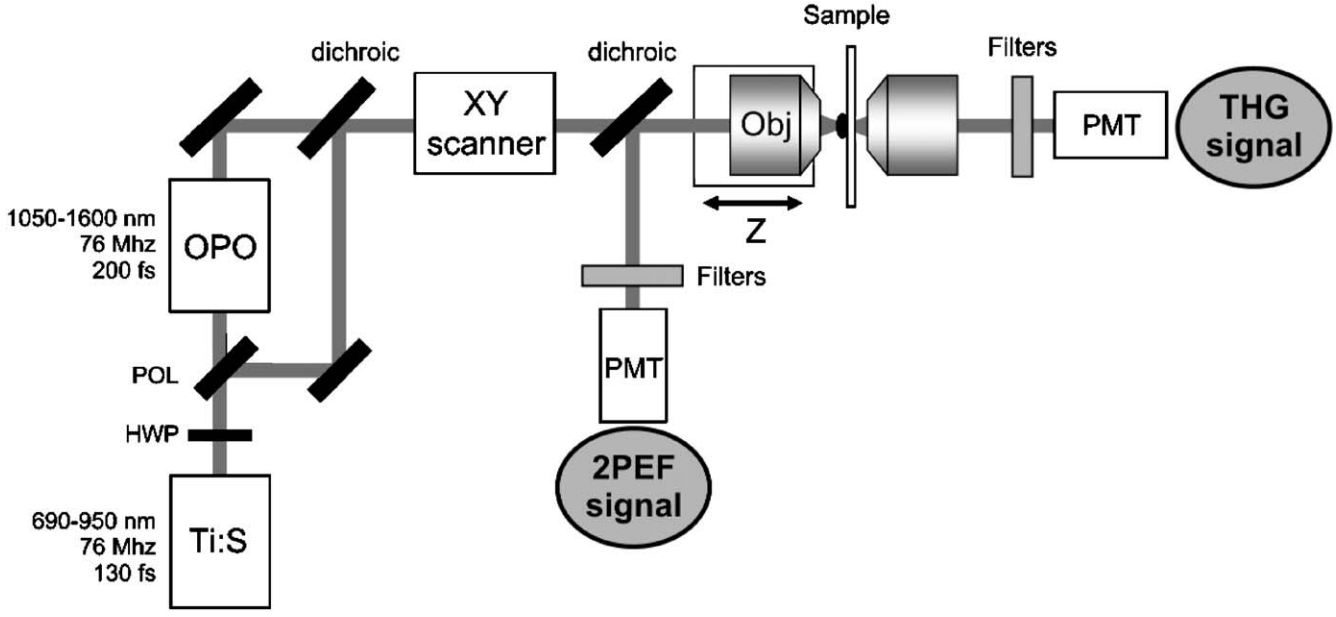

Fig. 1. Experimental setup. The output power from a titanium:sapphire oscillator (Ti:S) is modulated using a half-wave plate (HWP) and a polarizer (POL). The polarized beams are sent into an optical parametric oscillator (OPO) and directly into the scanning microscope. Mechanical shutters are used to select the OPO or the Ti:S beam (not shown). The excitation beam is scanned with galvanometers, and expanded to fill the back aperture of a water-immersion objective (Obj). Signals are detected by photon-counting photomultipliers modules (PMT) synchronized with the scanners. 2PEF is epidetected through the same objective and selected using a dichroic mirror and filters. THG light is detected in the transmitted direction through a condenser and selected using an interference filter.

ablations. 2PEF was epidetected when exciting GFP-expressing embryos at 920 nm. Alternatively, THG was detected in the transmitted direction when exciting unlabeled embryos at 1180 nm. In either case the signal of interest was selected using filters centered on the emission wavelength (Chroma). Images are presented in inverted contrast, and contrast-enhanced to outline the principal features.

Femtosecond pulse-induced ablation

For the ablations used in Fig. 5, 100 μm × 40 μm regions were processed by performing typically three line scans (100 μm long, 10–20 μm away from the vitelline membrane) in three successive planes separated 10–15 μm from one another. Laser power and scanning speed were chosen such that experimental conditions remained along the black dashed line in Fig. 2.

Cellularization speed measurements

Cellularization speed was estimated from image sequences by analyzing 1D-kymographs (i.e. space–time XT projections) obtained using MetaMorph (Universal Imaging Corporation). Kymographs were computed along the apico-basal axis over 10 μm-wide areas, which gave a typical precision of 0.05 μm/min. Fig. 4A is a compilation of data consistently obtained on wild-type embryos (using THG and transmitted-light microscopy) and on cytoskeleton-labeled (sGMCA) embryos.

Experimental characterization of femtosecond pulse-induced ablation

The interaction of high repetition rate (76 MHz) nanojoule femtosecond pulse trains with complex biological media has not been fully characterized yet; in particular, very few studies have focused on micro-dissections within developing embryos. In order to use this technique for studying embryo biomechanics, we first performed an experimental characterization of pulse-train effects on embryo tissue as a function of illumination parameters. Our experimental setup (Fig. 1 and methods) combines femtosecond pulse-induced ablation with MPM, by taking advantage of a single laser chain. We therefore used 2PEF and THG microscopy to characterize the effect of line scans on embryos. Pulse trains from a Ti:S oscillator (130 fs pulses, 76 MHz, $\lambda = 830$ nm) were focused inside live wild-type *Drosophila* embryos at stage 5 [32] of development. The beam was focused 5–15 μm beneath the vitelline membrane (other eggshells having been removed) using a 0.9 NA objective. Line scans of ~100 μm length were performed for different values of the average power at the sample surface (P_{ave}) and of the scanning speed (v_{scan}). We explored effects of average power and scan speed in the ranges 50–275 mW and 0.2–50 μm ms^{-1}, respectively. Previous studies of the effect of pulse trains on biological samples used a variety of illumination parameters such as pixel dwell time [24,26], number of scans [36] or fluence [37]. In order to facilitate the comparison of experimental

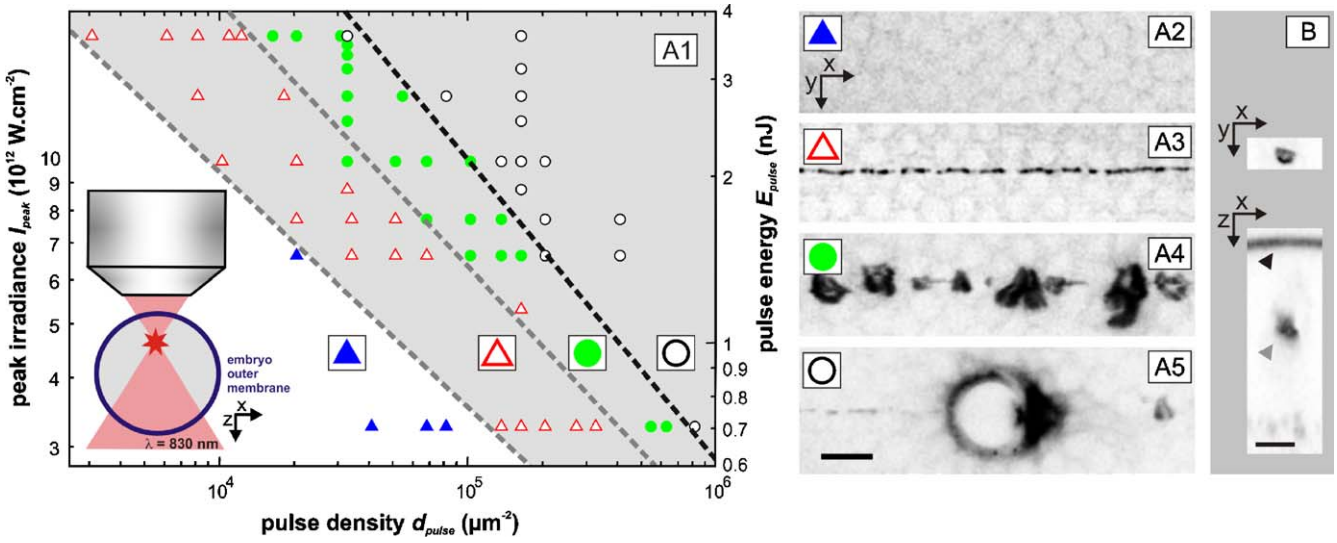

Fig. 2. (**A1**) Photo-induced effects of a 60–100 μm-long line scan in *Drosophila* embryos, as a function of irradiance I_{peak} (W cm^{-2}, vertical axis) and pulse density (number of pulses received per surface unit in μm^2). Experiments were performed on $n = 14$ embryos, and several points were recorded for each embryo. (**A2–A4**) Illustration of the four categories of the diagram (see text), corresponding to increasing pulse energy (or decreasing scanning speed). Images were recorded using 2PEF microscopy at lower excitation intensity. (**B**) Confined intravital ablation (gray arrowhead) performed 20 μm below the embryo vitelline membrane (black arrowhead). Scale bar: 10 μm.

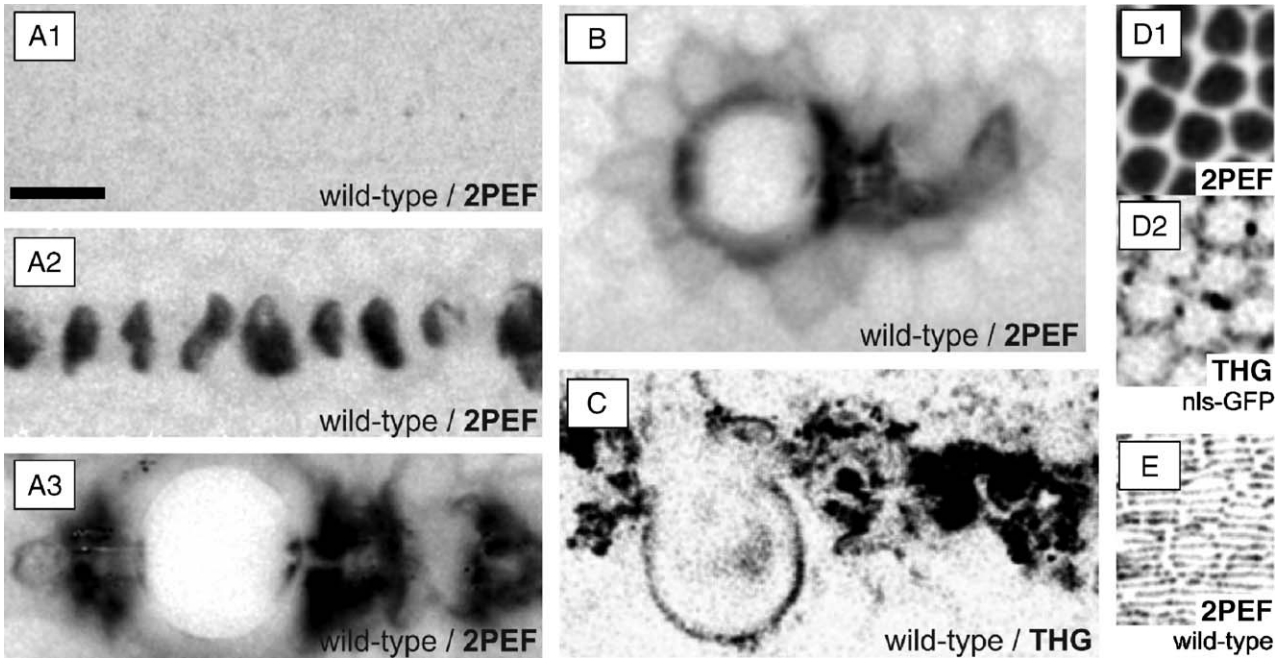

Fig. 3. (**A1–A3**) Comparison of the effect of single versus multiple line scans, for a constant peak irradiance and pulse density. (**A1**) A single line scan using conditions falling in the first category of the diagram (Fig. 2, filled triangles) induces no visible effect (single scan, $I_{peak} = 6.7 \times 10^{12}\,W\,cm^{-2}$, $d_{pulse} = 1.4 \times 10^{4}\,\mu m^{-2}$). (**A2**) Repeating 30 such scans with 500 ms delay between scans induces a series of microexplosions (30 scans, $I_{peak} = 6.7 \times 10^{12}\,W\,cm^{-2}$, $d_{pulse} = 4.1 \times 10^{5}\,\mu m^{-2}$). (**A3**) Increased photodestruction is observed when performing a single scan at slower speed (single scan, $I_{peak} = 6.7 \times 10^{12}\,W\,cm^{-2}$, $d_{pulse} = 4.1 \times 10^{5}\,\mu m^{-2}$). (**B**) When large bubbles are induced (Fig. 2, open circles), an increase in endogenous fluorescence is observed in cells immediately surrounding the targeted area. (**C**) THG image of a targeted region (Fig. 2, open circles) showing the presence of a gas bubble. (**D1**) 2PEF image of nuclei-labeled embryos (nls-GFP strain). (**D2**) Same region observed using THG microscopy, revealing perinuclear organelles. (**E**) Effect of a raster scan ("open triangles" category in Fig. 2) in a similar area on a wild-type embryo. This image illustrates that femtosecond pulses-induced effects occur first in cytoplasmic regions. Scale bar: 10 μm.

conditions, we propose to use here the peak irradiance I_{peak} and the pulse surface density d_{pulse} (i.e. number of pulses received per tissue surface unit). Assuming a FWHM beam size at the focal spot of $\lambda/(2NA)$, the expression of peak irradiance I_{peak} and pulse density d_{pulse} are related to the average power P_{ave}, the laser repetition rate $1/T$, the pulse duration τ_{pulse}, and the scan speed v_{scan}, as

$$I_{peak} \approx \frac{16 P_{ave} T NA^2}{\tau_{pulse}\,\pi \lambda^2} \quad \text{and} \quad d_{pulse} \approx \frac{2NA}{v_{scan} T \lambda}.$$

Our experimental conditions (Fig. 2), corresponded to I_{peak} ranging from 3×10^{12} to $2 \times 10^{13}\,W\,cm^{-2}$ (i.e. pulse energy ranging from 0.7 to 3.6 nJ), and d_{pulse} ranging from 3×10^{3} to 8×10^{5} pulses μm^{-2}. After each line scan, laser power was attenuated to ~12 mW ($I_{peak} 7 \times 10^{11}\,W\,cm^{-2}$), and the effect of the scan was immediately observed by recording a 2PEF image of the induced fluorescence in the targeted area. Alternatively, we sometimes used the OPO beam ($\lambda = 1180$ nm) to record a THG image of the tissue.

Line scan effects were qualitatively grouped into four categories illustrated in Figs. 2A1–A4. Category 1 (filled triangles) corresponds to no detectable effect when recording 2PEF images of embryo endogenous fluorescence. Category 2 (open triangles) corresponds to the onset of intense endogenous fluorescence (>7 times its original level) along the scan, and the possible occurrence of micro-explosions smaller than cell size (<5–6 μm in diameter) occurring first in the perinuclear region of the cytoplasm. This observation is also illustrated in Fig. 3E, which shows the effect of a raster scan under similar excitation conditions. The location of the fluorescent lesions can be compared with Figs. 3D1 and D2, which present images of an equivalent area in an intact, nuclei-labeled embryo. The strongest lesions may be related to the destruction of mitochondria, where optical breakdown was reported to occur first in similar experiments on individual cells [38]. Such a localization could be a signature of multiphoton absorption-enhanced ablation due to the presence of absorbing species, as recently reported [25,27]. Category 3 (filled circles) corresponds to the occurrence of micro-explosions larger than cell size (>5–6 μm), and

the possible formation of small bubbles collapsing before 5 s. Finally, category 4 (open circles) corresponds to the formation of large gas-filled bubbles ($>$ 5–6 μm) persisting for more than 5 s. In these illumination conditions, we also recorded a limited increase (3–4 times) of the endogenous fluorescence of cells immediately adjacent to the targeted region, as illustrated in Fig. 3B. This observed side effect may be related to a local metabolic stress [39]. We note that ablation-induced bubbles can efficiently be detected using THG microscopy (Fig. 3C) because of the contrast in optical properties (refractive index, nonlinear susceptibility) between the inside and the outside of the bubble. This is reminiscent of a previous observation that THG microscopy can be used to characterize optical breakdown-induced alterations in materials [40]. These observations were highly reproducible from one embryo to the other, and are summarized in the diagram of effects presented in Fig. 2A. A key benefit of femtosecond pulse-induced ablation for embryo studies is that the photodestructive effects bear a nonlinear dependence on excitation intensity. As a consequence, inner embryo structures can be processed without altering the outer membranes (Fig. 2B), which is critical to preserve embryo viability.

We also investigated the influence of experimental parameters including laser wavelength, number and periodicity of multiple scans, and embryo scattering properties. We found a relatively limited dependence of induced effects on laser wavelength in the range 830–920 nm (data not shown). As a consequence, an excitation wavelength of 920 nm is convenient for performing both ablations and 2PEF imaging of GFP-labeled embryos. We note that although we systematically used 76-MHz pulse trains, the pulse repetition rate likely has a critical influence: as previously suggested [36], we found it less effective to redistribute the total deposited energy into several scans instead of a single scan, especially when successive scans are separated by a time delay (illustrated in Fig. 3A). Finally, inner tissue dissection can be achieved by increasing the incident power to compensate for laser light scattering. However the maximum ablation depth depends on the embryo developmental stage, because embryos become more transparent as they develop. At stage 5 (before gastrulation), the inner regions of the embryos are very scattering [16] (yolk consisting of a high concentration of storage vesicles), which hampers deep micro-dissections. For example, micrometer-sized bubbles could be induced only up to 70 μm under the surface. At later stages (e.g. embryonic development completion, stage 16), similar effects could be obtained 100 μm under the surface (i.e. further than the embryo equator). All together, these observations enabled us to perform reproducible intravital micro-dissections in developing embryos.

Biological characterization of femtosecond pulse-induced ablation

As a nonlinear effect [36], multiphoton absorption leading to plasma-induced ablation is confined near the beam focus, which limits the spatial extent of the photodestructive effects. In addition, when using tightly focused femtosecond pulses, only a few nanojoules of energy are required to reach the peak irradiance necessary for tissue ablation. In comparison, other techniques of laser surgery require higher energy deposition by several orders of magnitude [17]. Finally, it is expected that femtosecond pulse-induced ablation results in localized dissection with limited thermal energy transfer or shock wave mechanical stress, causing minimal biological damage to surrounding cells [37,41]. This is supported by several studies of the photodamage induced by femtosecond pulses in cells and tissues [39]. The effect of nanojoule femtosecond pulses at high repetition rate (80 MHz) have been investigated ex vivo in ocular tissue by histological examination [26], in vivo in squid neurons by monitoring organelles dynamics around targeted areas [24], and in plant tissue using vital stains [21]. In addition, the temperature increase inside the focal volume has been shown to remain within physiological conditions, even for high irradiance and long exposure duration [42]. These experiments globally indicate that cell injury is confined to the targeted region, but little data is available regarding the spatial extent of the photoperturbation in vivo.

To gain insight into the effect of femtosecond pulses on developing embryos, we studied the influence of microdissections on the process of cellularization, a dynamical event of embryonic cells at the cellular blastoderm stage. This 1 h-long process occurs in some insects just before the cell movements of gastrulation and is related to conventional cytokinesis. The nuclei being initially distributed at the embryo periphery, cellularization involves simultaneous oocyte plasma membrane folding between all nuclei, eventually partitioning off each nucleus in a single cell [43] (Fig. 4B). Recent studies show that the rate and completion of cellularization front invagination appear as sensitive indicators of cytoskeleton integrity and dynamics [34,35]. In addition, cellularization speed is a sensitive probe of local temperature changes (Fig. 4A). We estimated the temperature dependence of this process by recording image sequences of developing embryos at physiologically relevant temperatures ranging from 19 to 27 °C. Cellularization speed was measured by kymograph analysis (space–time XT projections) of the image sequences, which provided a precision of 0.05–0.1 $\mu m\,min^{-1}$ (Fig. 4A). At 19 °C, cellularization exhibits three phases in control embryos: the slow phase (SP, ~0.3 μm/min), the early fast phase (EFP, ~0.6 μm/min) starting when the cellularization front reaches the

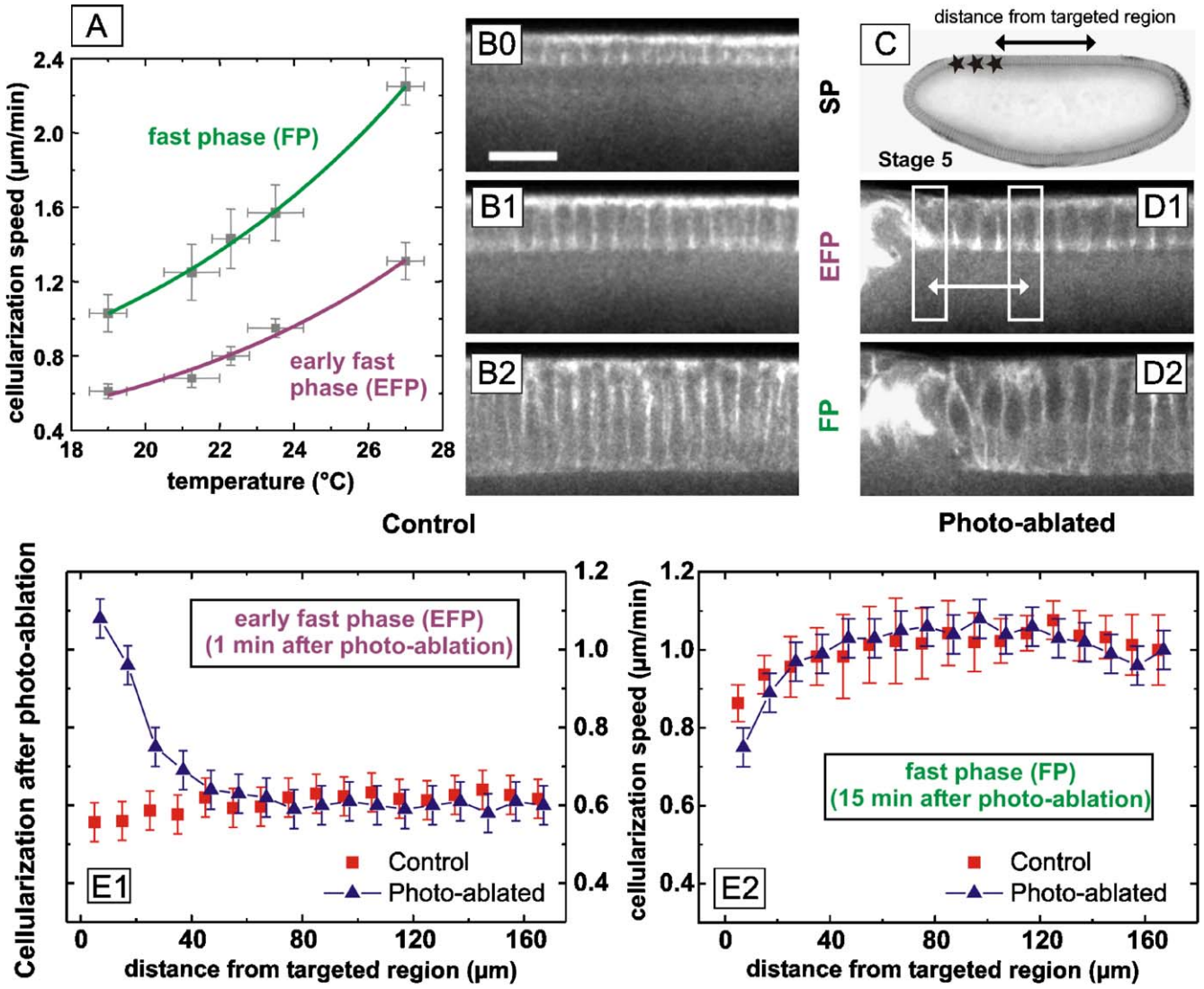

Fig. 4. Ablations induce minimal damage to local cytoskeleton dynamics. Cellularization speed in control embryos, exhibits three successive phases: a slow phase (SP, ~0.3 µm/min at 19 °C, **B0**), an early fast phase (EFP, ~0.6 µm/min at 19 °C, **B1**) and a fast phase (FP, ~1 µm/min at 19 °C, **B2**) after the cellularization front passes above the nuclei [34,35]. (**A**) Temperature dependence of cellularization speed in control embryos, measured at the middle of the dorsal side. (**B**) Cellularization in a control (sGMCA) embryo. (**C**) Embryo before ablation (anterior left, dorsal up). Stars indicate the targeted region. (**D**) Cellularization in an ablated embryo. (**E1, E2**) Cellularization speed in control and ablated embryos, as a function of distance from the targeted area. Photoablations were performed during EFP (**B1**, **D1**), and cellularization was monitored 1 min (**E1**) or 15 min (**E2**) after. Scale bar: 20 µm.

apical region of nuclei, and the fast phase (FP, ~1 µm/min) after the cellularization front passes above the basal part of nuclei. Between 19 and 27 °C, we measured the temperature dependence of cellularization rate to be typically 0.1 µm min^{-1} $°C^{-1}$ during EFP and 0.2 µm min^{-1} $°C^{-1}$ during FP. Given the precision of the analysis, we could easily detect local temperature changes of 1 °C.

We then monitored cellularization around ablated regions in GFP-labeled (sGMCA) embryos. Our experiments showed that cellularization still completed in cells adjacent to the targeted area (Fig. 4C). We could detect transient changes in cellularization speed over a limited distance (40 µm corresponding to 7–8 cells) and time (~10 min) (Fig. 4D). Factors that may account for this local perturbation include heating [42,44], metabolic stress [38], and perturbed integrity of the supracellular cytoskeleton network [35]. If heating is involved in this perturbation, Fig. 4A indicates that the temperature reached locally remains less than 26 °C, which corresponds to physiologically acceptable conditions for *Drosophila* embryos. In particular, cellularization rate is not temperature saturated in the observed conditions. Most importantly, (i) no change could be detected at distances larger than 40 µm from the ablation, and (ii) 15 min after laser ablation, cellularization rate was normal in cells immediately adjacent to the targeted

region, suggesting that heating plays only a marginal role (if any). Most likely, given the characteristics of the laser pulses used, the main factor accounting for the perturbation is the mechanical coupling between cells.

The key point of these observations is that this type of micro-dissection does not directly induce large-scale or long-term perturbation to cytoskeleton dynamics. Therefore, it can be considered to be a valid technique for studying dynamical processes and biomechanics within developing embryos.

Application: Modulation of morphogenetic movements

Recent studies have demonstrated that the manipulation of dynamic processes in live embryos using physical (non-genetic) means can complement genetic approaches and provide insight into embryo development. For example, temperature gradient application by micro-fluidics device [45] and UV laser-induced tissue ablation [46] were used to study *Drosophila* embryo development. Similarly, the combination of ultrashort pulse-induced ablation and nonlinear microscopy offers novel opportunities for investigating the relationships between embryo shape, mechanical structure, tissue deformations, and molecular signaling. In particular, we have recently reported that cell deformations involved in morphogenetic movements could induce gene expression during *Drosophila* embryo gastrulation, through a mechanical feedback process [47] possibly implied in the control of morphogenesis [48,49]. Specifically, the expression of *twist*, a fundamental gene of *Drosophila* early development which is involved in active cell deformations and in anterior gut track formation [50,51], appears to be sensitive to tissue deformations in gut precursor cells (Stomodeum Primordium, or SP cells) [47]. We reported how the combination of femtosecond pulse-induced ablation and nonlinear microscopy can be used to study this phenomenon [29]. We took advantage of the 3D confinement of femtosecond pulse-induced ablations to locally modify the embryo structural integrity, resulting in a modulation of morphogenetic movements. As depicted in Fig. 5, the photodestruction of a particular region of

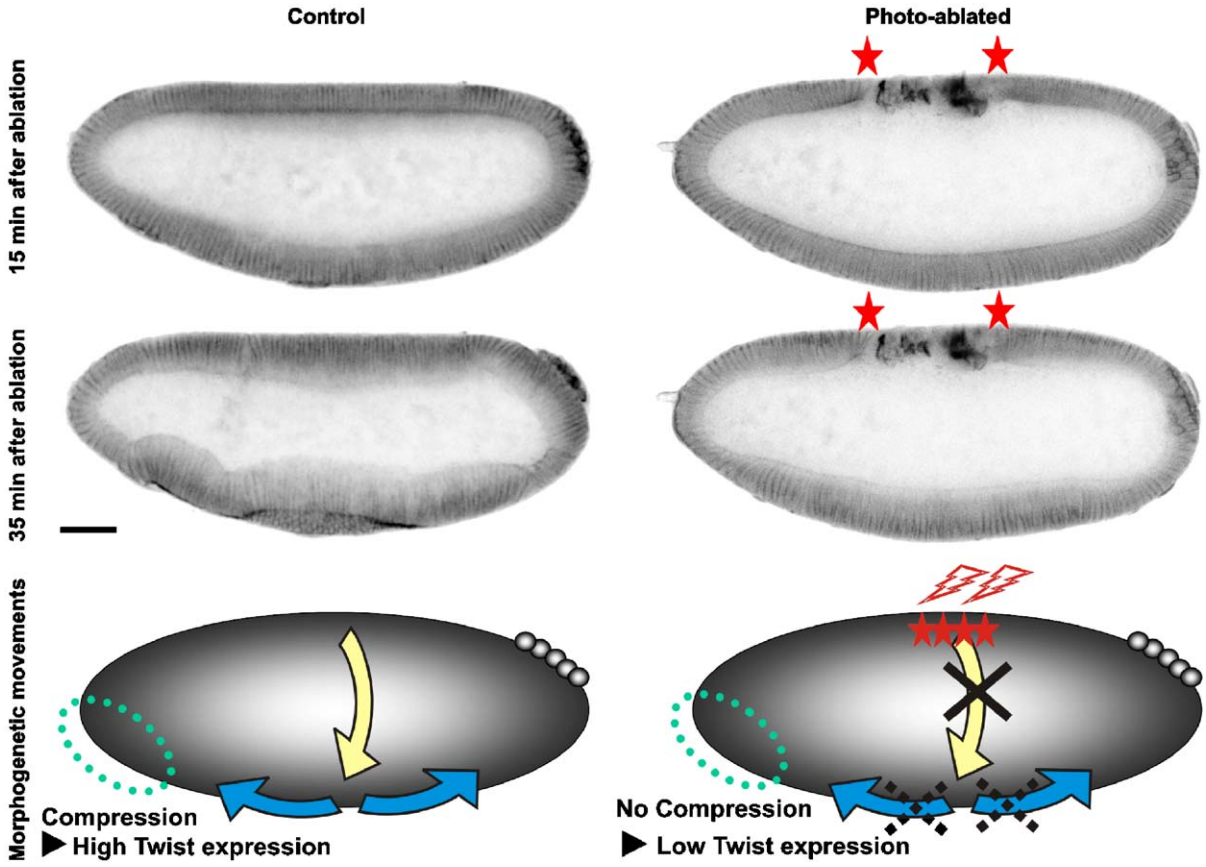

Fig. 5. Modulation of morphogenetic movements using femtosecond pulse-induced ablation. Photoablation of a $150 \times 40\,\mu m$ dorsal region (right, between stars) results in the disruption of morphogenetic movements coupled to the targeted area, as schematized in the bottom diagrams. In particular, a dorsal ablation remotely disrupts the compression of anterior pole cells (region within dotted ellipse). Anterior left, dorsal up. Scale bar: $50\,\mu m$.

the embryo results in a rapid (<10 min), long-range (>200 μm) modulation of morphogenetic movements connected to the targeted area. For example, targeting the most dorsal cells disrupt lateral cell movements originating from this region, and subsequent movements at the anterior pole of the embryo. In particular, a dorsal ablation remotely hampers the mechanical compression of SP cells (at the anterior pole). Combining this methodology with image sequence analysis and *twist* expression labeling in intact/ablated embryos revealed that there is a strong correlation between the deformation pattern of SP cells and the expression pattern of *twist* [29].

Discussion

The precise mechanisms of femtosecond laser interaction with complex biological media are still under extensive study, particularly in the case of high repetition rate (76 MHz), low energy (nJ) NIR pulses. Since the peak irradiance at the focal spot can reach values in the range of TW cm^{-2} when tightly focusing nanojoule femtosecond pulses, it is expected that multiphoton-mediated optical breakdown plays an important role in the experimental conditions used here. This process is presumably the main mechanism of laser energy deposition in low-absorbing tissues [37] and leads to plasma-induced tissue ablation [17,41]. However, local thermal and photochemical effects cannot be ruled out without further study. Nevertheless, our experiments showed that even large-scale ablations induce minimal perturbation to the adjacent cells, as revealed by cytoskeleton dynamics (Fig. 4) and gene expression patterns (not shown).

In contrast, local intra-embryonic ablations result in a rapid modulation of large-scale morphogenetic processes that is likely related to the perturbation of the embryo mechanical integrity. The natural combination of femtosecond pulse-induced ablation and MPM therefore holds promise for studying the biomechanics of embryo development. For example, we observed that the size and location of ablated regions have a critical influence on the resulting perturbation of morphogenetic processes. This all-optical methodology may prove complementary to genetic approaches, by providing the unique ability to target specific structures instead of interfering with specific genes. For example, this approach could be used for studying the mechanical coupling between morphogenetic movements, or for elucidating the relative role of active and passive cell deformations involved in morphogenesis. More generally, it provides a direct means to study the interplay between cell deformations and molecular signaling, and should find many applications in cell and developmental biology.

Acknowledgements

The authors thank C. Schaffner, M. Bierry, J.-M. Sintes and X. Solinas for expert technical help, and D.P. Kiehart and R.A. Montague for the gift of the sGMCA transgenic line. This work was supported by the Association pour la Recherche sur le Cancer and the Délégation Générale pour l'Armement.

Zusammenfassung

Femtosekunden-Puls-induzierte Mikroentwicklungssteuerung von lebenden *Drosophila* Embryonen

Der Effekt von Femtosekunden-Pulsen auf die Gastrulation von *Drosophila* Embryonen wurde mit Hilfe von Zwei-Photonen Fluoreszenz- und THG-Mikroskopie charakterisiert. Femtosekunden-Pulse können dazu verwendet werden, kontrollierte, intravitale Mikrodissektionen durchzuführen, die die strukturelle Integrität des Embryos verändern, aber die Cytoskelettdynamik in den umgebenden Zellen nicht wesentlich beeinflussen. Mit Hilfe dieser gezielten Ablationen können Zellbewegungen in sich entwickelnden Embryonen von fern beeinflusst werden. Die direkte Verbindung von Femtosekunden-Puls-induzierter Ablation mit nichtlinearer Mikroskopie kann dazu verwendet werden, in vivo den Effekt von Formveränderungen von Zellen und Geweben zu untersuchen.

Schlüsselwörter: Femtosekunden-Puls-induzierte Ablation; Zwei-Photonen Fluoreszenz-Mikroskopie; THG-Mikroskopie; *Drosophila* embryonal Entwicklung

References

[1] Denk W, Strickler JH, Webb WW. Two-photon laser scanning fluorescence microscopy. Science 1990;248:73–6.
[2] Zipfel WR, Williams RM, Webb WW. Nonlinear magic: multiphoton microscopy in the biosciences. Nat Biotechnol 2003;21:1369–77.
[3] Charpak S, Mertz J, Beaurepaire E, Moreaux L, Delaney K. Odor-evoked calcium signals in dendrites of rat mitral cells. Proc Natl Acad Sci USA 2001;98:1230–4.
[4] Mertz J. Nonlinear microscopy: new techniques and applications. Curr Opin Neurobiol 2004;14:610–6.
[5] Svoboda K, Tank DW, Denk W. Direct measurement of coupling between dendritic spines and shafts. Science 1996;272:716–9.
[6] Cahalan MD, Parker MD, Wei SH, Miller MJ. Two-photon tissue imaging: seeing the immune system in a fresh light. Nat Rev Immunol 2002;2:872–80.
[7] Stroh M, Zimmer JP, Duda DG, Levchenko TS, Cohen KS, Brown EB, et al. Quantum dots spectrally distinguish multiple species within the tumor milieu in vivo. Nat Med 2005;11:678–82.

[8] Squirrell JM, Wokosin DL, White JG, Bavister BD. Long-term two photon fluorescence imaging of mammalian embryos without compromising viability. Nat Biotechnol 1999;17:763–7.
[9] Freund I, Deutsch M. Second-harmonic microscopy of biological tissue. Opt Lett 1986;11:94–6.
[10] Barad Y, Eisenberg H, Horowitz M, Silberberg Y. Nonlinear scanning laser microscopy by third harmonic generation. Appl Phys Lett 1997;70:922–4.
[11] Cheng J-X, Xie XS. Coherent anti-Stokes Raman scattering microscopy: instrumentation, theory, and applications. J Phys Chem B 2004;108:827–40.
[12] Duncan MD, Reintjes J, Manuccia TJ. Scanning coherent anti-Stokes Raman microscope. Opt Lett 1982;7:350–2.
[13] Oron D, Yelin D, Tal E, Raz S, Fachima R, Silberberg Y. Depth-resolved structural imaging by third-harmonic generation microscopy. J Struct Biol 2004;147:3–11.
[14] Squier JA, Müller M, Brakenhoff GJ, Wilson KR. Third harmonic generation microscopy. Opt Express 1998;3: 315–24.
[15] Sun C-K, Chu S-W, Chen S-Y, Tsai T-H, Liu T-M, Lin C-Y, et al. Higher harmonic generation microscopy for developmental biology. J Struct Biol 2004;147:19–30.
[16] Débarre D, Supatto W, Farge E, Moulia B, Schanne-Klein M-C, Beaurepaire E. Velocimetric third-harmonic generation microscopy: micrometer-scale quantification of morphogenetic movements in unstained embryos. Opt Lett 2004;29:2881–3.
[17] Niemz MH. Laser–Tissue Interactions: Fundamentals and Applications. Berlin: Springer; 2004.
[18] Sugar A. Ultrafast (femtosecond) laser refractive surgery. Curr Opin Ophthalmol 2002;13:246–9.
[19] Tsai PS, Friedman B, Ifarraguerri AI, Thompson BD, Lev-Ram V, Schaffer CB, et al. All-optical histology using ultrashort laser pulses. Neuron 2003;39:27–41.
[20] Yanik MF, Cinar H, Cinar HN, Chisholm AD, Jin Y, Ben-Yakar A. Neurosurgery: functional regeneration after laser axotomy. Nature 2004;432:822.
[21] Tirlapur UK, König K. Femtosecond near-infrared laser pulses as a versatile non-invasive tool for intra-tissue nanoprocessing in plants without compromising viability. Plant J 2002;31(3):365–74.
[22] König K, Riemann I, Fritzsche W. Nanodissection of human chromosomes with near-infrared femtosecond laser pulses. Opt Lett 2001;26:819–21.
[23] Tirlapur UK, König K. Cell biology: targeted transfection by femtosecond laser. Nature 2002;418:290–1.
[24] Galbraith JA, Terasaki M. Controlled damage in thick specimens by multiphoton excitation. Mol Biol Cell 2003;14:1808–17.
[25] Heisterkamp A, Maxwell IZ, Mazur E, Underwood JM, Nickerson JA, Kumar S, et al. Pulse energy dependence of subcellular dissection by femtosecond laser pulses. Opt Express 2005;13:3690–6.
[26] König K, Krauss O, Riemann I. Intratissue surgery with 80 MHz nanojoule femtosecond laser pulses in the near infrared. Opt Express 2002;10:171–6.
[27] Sacconi L, Tolic-Nørrelykke IM, Antolini R, Pavone FS. Combined intracellular three-dimensional imaging and selective nanosurgery by a nonlinear microscope. J Biomed Opt 2005;10:14002.
[28] Watanabe W, Arakawa N, Matsunaga S, Higashi T, Fukui K, Isobe K, et al. Femtosecond laser disruption of subcellular organelles in a living cell. Opt Express 2004;12:4203–13.
[29] Supatto W, Débarre D, Moulia B, Brouzes E, Martin JL, Farge E, et al. *In vivo* modulation of morphogenetic movements in *Drosophila* embryos with femtosecond laser pulses. Proc Natl Acad Sci USA 2005;102: 1047–52.
[30] Kiehart DP, Galbraith CG, Edwards KA, Rickoll WL, Montague RA. Multiple forces contribute to cell sheet morphogenesis for dorsal closure in *Drosophila*. J Cell Biol 2000;149:471–90.
[31] Davis I, Girdham CH, O'Farrell PH. A nuclear GFP that marks nuclei in living *Drosophila* embryos: maternal supply overcomes a delay in the appearance of zygotic fluorescence. Dev Biol 1995;170:726–9.
[32] Wieschaus E, Nusslein-Volhard C. Looking at embryos. *Drosophila*, a practical approach. Oxford: Oxford University Press; 1998.
[33] Davis I. Visualizing fluorescence in *Drosophila* – optimal detection in thick specimen. Protein localization by fluorescence microscopy: a practical approach. Oxford: Oxford University Press; 2000.
[34] Royou A, Field C, Sisson JC, Sullivan W, Karess R. Reassessing the role and dynamics of nonmuscle myosin II during formation in early *Drosophila* embryos. Mol Biol Cell 2004;15:838–50.
[35] Thomas JH, Wieschaus E. src64 and tec29 are required for microfilament contraction during *Drosophila* cellularization. Development 2003;131:863–71.
[36] Hopt A, Neher E. Highly nonlinear photodamage in two-photon fluorescence microscopy. Biophys J 2001;80: 2029–36.
[37] Oraevsky AA, Silva LBD, Rubenchik AM, Feit MD, Glinsky ME, Perry MD, et al. Plasma mediated ablation of biological tissues with nanosecond-to-femtosecond laser pulses: relative role of linear and nonlinear absorption. IEEE J Select Topics Quantum Electron 1996;2: 801–9.
[38] Oehring H, Riemann I, Fischer P, Halbhuber K-J, König K. Ultrastructure and reproduction behaviour of single CHO-K1 cells exposed to near infrared femtosecond laser pulses. Scanning 2000;22:263–70.
[39] König K, Tirlapur UK. Cellular and subcellular perturbations during multiphoton microscopy. Confocal and two-photon microscopy: foundations, applications, and advances. New York: Wiley-Liss; 2002.
[40] Squier JA, Müller M. Third-harmonic generation imaging of laser-induced breakdown in glass. Appl Opt 1999;38:5789–94.
[41] Vogel A, Noack J, Nahen K, Theisen D, Bush S, Parlitz U, et al. Energy of optical breakdown in water at nanosecond to femtoseconds time scales. Appl Phys B 1999;68:271–80.
[42] Schönle A, Hell S. Heating by absorption in the focus of an objective lens. Opt Express 1998;23:325–7.
[43] Foe ME, Odell MO, Edgar BA. Mitosis and gastrulation in the *Drosophila* embryo: point and conterpoint. The

development of *Drosophila melagonaster*. New York: Cold Spring Harbor Laboratory Press; 1993.
[44] Schaffer C, Garcia J, Mazur E. Bulk heating of transparent materials using a high repetition-rate femtosecond laser. Appl Phys A 2003;76:351–4.
[45] Lucchetta EM, Lee JH, Fu LA, Patel NH, Ismagilov RF. Dynamics of *Drosophila* embryonic patterning network perturbed in space and time using microfluidics. Nature 2005;434:1134–8.
[46] Hutson MS, Tokutake Y, Chang M- S, Bloor JW, Venakides S, Kiehart DP, et al. Forces for morphogenesis investigated with laser microsurgery and quantitative modeling. Science 2003;300:145–9.
[47] Farge E. Mechanical induction of Twist in the *Drosophila* foregut/stomodeal primordium. Curr Biol 2003;13:1365–77.
[48] Brouzes E, Farge E. Interplay of mechanical deformation and patterned gene expression in developing embryos. Curr Opin Genet Dev 2004;14:367–74.
[49] Brouzes E, Supatto W, Farge E. Is mechano-sensitive expression of twist involved in mesoderm formation? Biol Cell 2004;96:471–7.
[50] Leptin M. Gastrulation in *Drosophila*: the logic and the cellular mechanims. EMBO J 1999;18:3187–92.
[51] Reuter R, Grunewald B, Leptin M. A role for the mesoderm in endodermal migration and morphogenesis in *Drosophila*. Development 1993;119:1135–45.